

# Plasmonic Coupler for Silicon-Based Micro-Slabs to Plasmonic Nano-Gap Waveguide Mode Conversion Enhancement

Y. Liu, Y. Lai, *Fellow, OSA*, and K. Chang, *Fellow, IEEE*

**Abstract**—We investigate a short ( $\sim 1.5 \mu\text{m}$ ) “partially” corrugated tapered waveguide for silicon-based micro-slab waveguide to plasmonic nano-gap waveguide mode conversion at the optical communication frequency. The structure is designed to achieve more precise mode matching between the silicon slabs and plasmonic waveguides. High transmission efficiencies up to 87%  $\sim$  98% have been demonstrated numerically. The results show that the corrugated structure should not only be helpful for realizing full on-chip silicon plasmonic devices but also a good choice for mode coupling enhancement from dielectric waveguides to plasmonic waveguides. Meanwhile, we point out that the coupling mechanism reported here is different from that achieved by exciting surface plasmon polaritons (SPPs) at metal surfaces reported in the literature [18], [19].

**Index Terms**—Couplers, plasmonic coupler, plasmonic waveguides, silicon based plasmonic coupler, silicon photonics.

## I. INTRODUCTION

WITH the advances of nano fabrication technologies, plasmonic waveguide devices have attracted intensive research interest in recent years mainly due to their strong optical confinement property at the scale that is much smaller than the free space optical wavelength. Such field confinement property provides a promising platform for the implementation of nano-metallic devices for optical communication applications. Among all the required new technologies, efficient light coupling is one of the important issues for the design of plasmonic gap waveguides. Since the effective index of  $\text{TM}_0$  plasmonic mode is higher than the material indices of the waveguiding structure, the efficient coupling from waveguide mode to plasmonic mode becomes more difficult, especially when the effective mode index difference between the conventional waveguide mode and the plasmonic mode is large (i.e. mode mismatch). So far, there are a couple literatures discussing the excitation of the non-silicon filled plasmonic gap waveguide

mode by using a plasmonic gap taper [1], a nano-antenna [2], a multi-section coupler [3] and a silicon slot waveguide [4]. However, none of these structures are aimed at the mode coupling of silicon filled plasmonic gap waveguides. To distinguish the complexity between silicon-based and silica-based plasmonic gap waveguide coupling via a slab waveguide, the effective mode index  $n_{\text{eff}}$  versus the waveguide width of the slab fundamental TM mode, the plasmonic  $\text{TM}_0$  mode and the plasmonic  $\text{TM}_2$  mode are plotted in Fig. 1(a) and (b) for the silicon-based case and the silica-based case respectively. According to [1], due to the structure symmetry of the considered problem, the symmetry nature of the modes plays an important role here for mode coupling. Since the excitation mode (the slab fundamental TM mode) is an even TM mode, only its nearby even plasmonic TM modes, plasmonic  $\text{TM}_0$  and  $\text{TM}_2$ , will be excited. Therefore, we just need to consider the mode coupling between the slab fundamental TM mode and plasmonic  $\text{TM}_0$ ,  $\text{TM}_2$  modes. This symmetry property can also be verified from  $H_z$  field profiles along  $y$  axis shown in Fig. 1(c) and (d). As shown in Fig. 1(a) and (c), one can see that most power of the fundamental TM mode of the silicon micro-slab will be coupled into the plasmonic  $\text{TM}_2$  mode rather than the plasmonic  $\text{TM}_0$  mode because of the presence of the closer plasmonic  $\text{TM}_2$  mode and the larger effective index difference between the slab fundamental TM mode and plasmonic  $\text{TM}_0$  mode. On the contrary, from Fig. 1(b) and (d), one can observe that the fundamental TM mode of the silica micro-slab is easier to be coupled into the plasmonic  $\text{TM}_0$  mode than the plasmonic  $\text{TM}_2$  mode as the effective index of the slab fundamental is closer to that of plasmonic  $\text{TM}_0$  mode. This is why the high efficiency conversion between the fundamental TM mode of a micron/sub-micron silicon slab and the plasmonic  $\text{TM}_0$  mode of a plasmonic gap waveguide is challenging in order to directly integrate the slab waveguide with the light source from an optical fiber or an on-chip laser for efficient light coupling.

In the microwave regime, corrugated metal structures have long been proposed and utilized as waveguide mode converters between conventional guided modes [5], surface wave assisted structures [6], slow-wave structures [7] or filters [8]. In recent years, they draw attentions again in the emergent researches on slow-light and THz applications [9], for similar purposes such as dispersion controlling [10] and the so called “spoof” or “designer” surface plasmon assisted structures operating at low THz frequencies [11]–[14], which are actually surface waves existing on inductive corrugated surfaces formed by perfect

Manuscript received December 23, 2012; revised March 14, 2013; accepted March 30, 2013. Date of publication April 12, 2013; date of current version April 26, 2013. This work was supported in part by NSC, Taiwan under the program number NSC-095-SAF-I-564-029-TMS, bp and SGI, USA.

Y. Liu and K. Chang are with Department of Electrical and Computer Engineering, Texas A&M University, College Station, TX 77843 USA (e-mail: ylgogogo@tamu.edu; chang@ece.tamu.edu).

Y. Lai is with Department of Photonics, National Chiao-Tung University, Hsinchu 300, Taiwan (e-mail: yclai@mail.nctu.edu.tw).

Color versions of one or more of the figures in this paper are available online at <http://ieeexplore.ieee.org>.

Digital Object Identifier 10.1109/JLT.2013.2257686

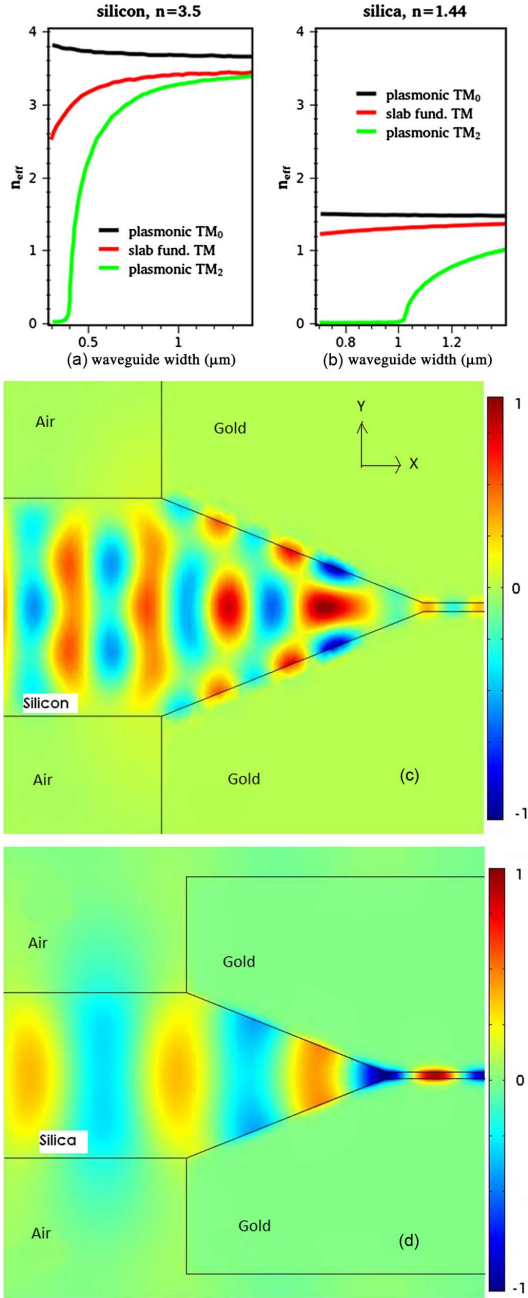


Fig. 1. Effective mode indices of plasmonic  $TM_0$  (black), slab fundamental TM (red) and plasmonic  $TM_2$  (green) modes for (a) silicon and (b) silica based slab waveguides and plasmonic gap waveguides. The  $H_z$  field coupling from a  $1.25 \mu\text{m}$  slab waveguide to  $50 \text{ nm}$  plasmonic gap waveguide with a  $1.5 \mu\text{m}$  taper for: (c) silicon based waveguides and (d) silica ( $\text{SiO}_2$ ) based waveguides. In (c), one can observe that most power is coupled into the plasmonic  $TM_2$  mode instead of the plasmonic  $TM_0$  mode (3.7%). A large amount of power is reflected at the gap size  $\sim 0.4 \mu\text{m}$  where the plasmonic  $TM_2$  mode becomes cutoff. In (d) one can observe that more power is coupled into the plasmonic  $TM_0$  mode (81.7%) rather than the plasmonic  $TM_2$  mode.

electrical conductors (PEC) described in Electromagnetics books [6], [7].

Recently, grooved metal sidewalls [18] (or another name, corrugated horn structure [19]) with  $6.2 \mu\text{m}$  input opening for metal-silicon-metal plasmonic gap waveguide coupling is reported with maximum 72% coupling efficiency. The coupling is achieved by exciting SPPs (Surface Plasmon Polaritons) at

metal surfaces [19] with TM polarized light thus the groove number will affect the transmission efficiency dramatically (Fig. 2 in [18]). In addition, the structure requires that (1) SPPs generated by adjacent grooves are in phase and (2) the incident lights falling on each groove are in phase for higher coupling efficiency. Therefore the corrugated metal surfaces have to be tapered at a specific angle ( $90^\circ - 32^\circ = 58^\circ$  in [18], [19]) and the groove distance has to be kept at  $2\lambda_{\text{SPP}}$  once the metal material is decided. These restrictions may somehow constrain the coupler design freedom by that approach.

Unlike open corrugated structures [12]–[14], [16], the waveguide dispersion of a corrugated waveguide (a closed structure), as shown in Fig. 2(a), can extend across the light line [5], [7], [10], [15], [17]. This in principle can be utilized in the coupler design to transform the waveguide guided mode ( $\beta < k$ ) across the light line to match the plasmonic mode with  $\beta > k$ . Here  $k$  is the wave number for the dielectric sandwiched between the grooved metal plates. As mentioned above, a corrugated metallic waveguide is known to be able to serve as a mode converter [5] between conventional guided modes due to its dispersion engineerable structure and low attenuation characteristics [15] at the microwave frequency. However, there is still no literature discussing the use of corrugated waveguide for optical guided mode to plasmonic mode coupling. In addition, at the optical frequency, metal is no longer a perfect conductor and the signal propagation loss is considerable especially when the corrugated metal structure is incorporated in the design. Therefore, whether a metallic corrugated coupler with high coupling efficiency is feasible for conventional guided mode to plasmonic mode conversion at the optical regime still requires further investigation, which is the main objective of the present work.

In this paper, a short ( $\sim 1.5 \mu\text{m}$ ) gold “partially” corrugated tapered waveguide for mode coupling enhancement at the  $1550 \text{ nm}$  optical communication wavelength between a  $1.25 \mu\text{m}$  silicon micro-slab and a plasmonic nano-gap waveguide is designed and analyzed for the first time. The coupling efficiency is examined to be able to reach 86%  $\sim$  98% with the plasmonic waveguide gap size ranging from  $20 \text{ nm}$  to  $300 \text{ nm}$ , which is comparable to or even higher than that of the previously referred non-silicon and silicon based cases. Finally, for comparison, we also use silver as the metal material in the design for different-size plasmonic gap waveguide coupling. The simulation results show that around 90% coupling efficiency on average can be achieved by using the corrugated tapered waveguide without the need to set the groove distance to be  $2\lambda_{\text{SPP}}$ , which directly proves that the coupling mechanism of the corrugated waveguide studied here is different from that of the grooved metal sidewalls [18] or the corrugated horn structure [19].

## II. DESIGN AND ANALYSIS

Fig. 2(a) shows a PEC periodic corrugated metallic parallel plate waveguide and its dispersion diagrams [7]. The period of the corrugation, the depth of the tooth, the width of the dielectric tooth, and the vertical distance between metal teeth are represented by  $p$ ,  $h$ ,  $t$  and  $g$  respectively, as depicted in the inset figure. One can see the corrugated waveguide can have modes across the light line [5], [7], [15], [17]. Although the dispersion

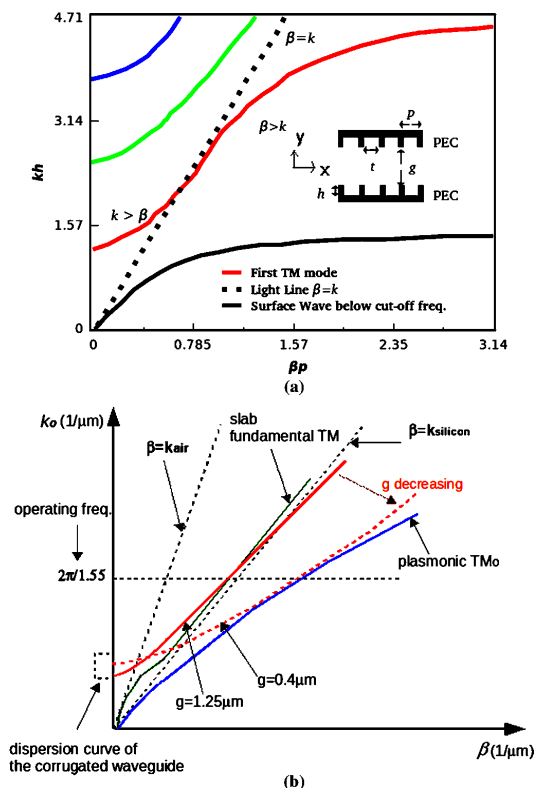


Fig. 2. (a) Dispersion diagram of a corrugated parallel-plate waveguide. As shown in the red line, the waveguide can have modes with both  $\beta > k$  and  $\beta < k$ . Blue and green lines represent higher order TM modes. (b) Schematic diagram for the design idea.

curves in Fig. 2(a) is based on PEC corrugation as a periodic system ( $p \sim \lambda_g$ ) and its dispersion relation is different from PEC corrugation as a uniform systems ( $p \ll \lambda_g$ ) [7], the relation between waveguide dispersion and the structure parameters ( $p$ ,  $h$ ,  $t$  and  $g$ ) for these two cases still share the same features. Fig. 3 shows the partially corrugated taper for the silicon filled plasmonic gap waveguide coupling. The width of the silicon slab  $w_1$  is set to be  $1.25 \mu\text{m}$  and the gap of the plasmonic metal-silicon-metal waveguide  $w_2$  is set to be  $20 \text{ nm}$  in Fig. 3(a),  $50 \text{ nm}$  in Fig. 3(b) and  $300 \text{ nm}$  in Fig. 3(c) respectively. In the design simulation, the relative permittivity for silicon is  $\epsilon_{\text{si}} = 12.25$  while the complex relative permittivity of the metal (gold) is  $\epsilon_{\text{Au}} = -93.0 + 11.0i$  determined by the Lorenz-Drude model [20]. The simulation work is done by the commercial 2D Finite Element software, which is also the approach used in [18], [19]. The accuracy of the 2D FEM is compared with the coupling efficiency calculated by 2D FDTD published in [1], which is a silica-based case with  $6 \mu\text{m}$  taper and  $50 \text{ nm}$  gap. In [1], the calculated coupling efficiency is reported to be  $\sim 70\%$  and our result based on 2D FEM simulation is  $69.3\%$ . The error is quite small in this case. However, for the silicon-based case, the numerical results generated by the open source FDTD code (MEEP) cannot converge well due to the staircasing approximation [21] introduced at the material interfaces with a large index contrast between the positive real part of the silicon and the negative real part of the metal. In contrast, for FEM, no staircasing approximation is required at the silicon-metal interfaces. Thus the field boundary conditions at the material interfaces can

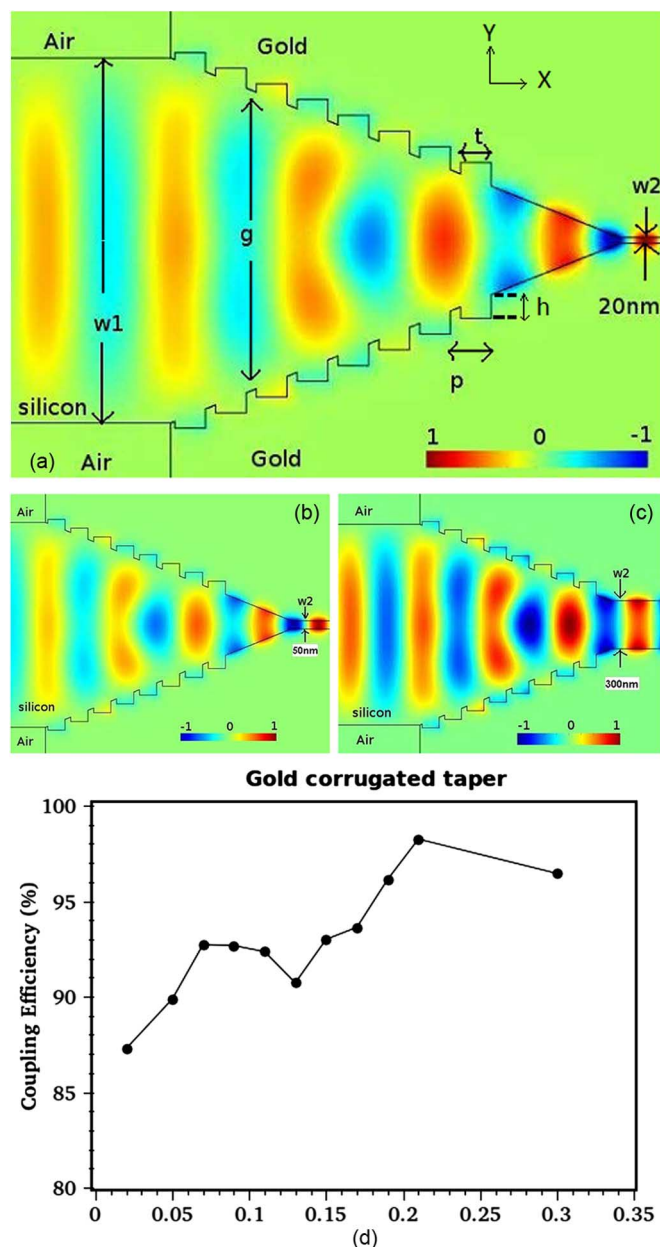


Fig. 3.  $1.25 \mu\text{m}$  ( $w_1$ ) silicon slab to gold plasmonic gap waveguide coupling with the plasmonic waveguide width  $w_2 =$  (a)  $20 \text{ nm}$ , (b)  $50 \text{ nm}$  and (c)  $300 \text{ nm}$ ; the Hz fields are plotted. The coupling efficiencies are  $\sim 87\%$ ,  $\sim 89\%$  and  $\sim 96\%$  respectively. (d) Plot of the coupling efficiency versus the plasmonic waveguide gap size.

be treated precisely and the meshes in the nano gap can be extremely refined to achieve high accuracy. Based on the above facts, previous literature [22] and our study [23], FEM should be more suitable than FDTD for plasmonic related problems especially when high material index contrast is involved.

In the design, the corrugation period  $p$  ( $\sim 0.14 \mu\text{m}$ ) is comparable to the effective wavelength  $\lambda_g$  ( $\sim 0.44 \mu\text{m}$ ) of the slab fundamental mode and thus the formulation for the uniform system is not applicable here. In addition, since finite corrugation periods are incorporated in the design, strictly speaking the corrugated taper cannot be considered as a periodic structure. Nevertheless, the dispersion relation for periodic systems still can provide a basic idea to decide the size of  $p$ ,  $h$  and  $t$  for the

effective mode index of the corrugated waveguide that matches the effective index of the fundamental slab TM mode at the input end with  $g = 1.25 \mu\text{m}$  and matches the effective index of the plasmonic  $\text{TM}_0$  mode with  $g \approx 0.4 \mu\text{m}$  around which the plasmonic  $\text{TM}_2$  mode is cut off, as shown in Fig. 1(a). In the design,  $p$ ,  $t$  and the taper length are set to be around  $0.14 \mu\text{m}$ ,  $0.1 \mu\text{m}$  and  $1.5 \mu\text{m}$  respectively. With given  $h$  and  $g$ ,  $\beta$  is then estimated by (1) [7].

$$\frac{p}{t} \frac{\sqrt{\beta^2 - k^2} \tanh\left(\frac{g}{2} \sqrt{\beta^2 - k^2}\right)}{k \operatorname{sinc}^2\left(\beta \frac{t}{2}\right)} = \tan(kh) \quad (1)$$

Here,  $k$  is the wave number for the dielectric sandwiched by the grooved metal plates and the value of  $h$  can be slightly optimized for better performance. According to (1), for a specific operating frequency (that is, for a specific  $k_0$ ),  $\beta$  increases as  $g$  decreases, as shown in Fig. 2(b). Therefore, as the slab TM mode passes through the corrugated region of the taper, it is transformed gradually into the mode with  $\beta > k$  that can match the plasmonic  $\text{TM}_0$  mode ( $\beta > k$ ) at the input of the non-corrugated taper. The reason why the taper is made “*partially*” corrugated is that only plasmonic  $\text{TM}_0$  mode exists when the metallic gap size drops below  $\sim 0.4 \mu\text{m}$ , as illustrated in Fig. 1(a). Under this situation, the loss will increase when the plasmonic  $\text{TM}_0$  mode keeps propagating on corrugated surfaces since the fields of the mode now concentrate more on the metal surfaces.

Based on the FEM simulation, the coupling efficiencies for 20 nm to 300 nm metal-silicon-metal gaps, as shown in Fig. 3(d), range from  $\sim 87\%$  to  $\sim 98\%$ , which proves that the corrugated waveguide structure can serve as the waveguide mode converter at the optical frequency with low attenuation as described in [15]. This is because most of the fields in the corrugated part of the taper are still confined at the waveguide center, as shown in Fig. 3(a)–(c). This fact directly proves that the coupling mechanism of the corrugated waveguide discussed here is not based on the excitation of SPPs on grooved metal surfaces shown in [18], [19]. Actually, according to [7], as a closed structure, the mode field pattern of the corrugated waveguide shown in Fig. 2(a) is of the form of hyperbolic sinusoidal functions ( $j/k_y \cosh(k_y y) e^{-j\beta x}$  for both  $H_z$  and  $E_y$  of symmetric TM mode) for both  $\beta > k$  and  $\beta < k$ . This is also true for the structure (closed structure as well) of our design, which supports that the field confined in the corrugated taper is not evanescent wave. This is why the propagation loss is low in the corrugated region of our design.

For the purpose of mechanism and performance comparison, the coupling efficiencies for silver based plasmonic gap waveguides with different gap sizes are provided in Fig. 4(b). The relative permittivity used here is  $\varepsilon_{\text{Ag}} = -143.49 + 9.52i$  [20], of which the imaginary part is larger than that used in [18] (i.e.  $\operatorname{Im}[(0.144 + 11.366i)^2] = -129.16 + 3.27i = 3.27$ ). According to Fig. 4(b), the overall coupling efficiency is obviously higher than the previous results (Fig. 8(a) in [18]). For the 50 nm silver plasmonic gap waveguide shown in Fig. 4(a), the coupling efficiency is  $\sim 93\%$  with 8 grooves, which is also much higher than the result reported in [18] ( $\sim 50\%$  with 4 grooves). Also note that the groove distance shown in Fig. 4(a) is  $0.15 \mu\text{m}$  (much

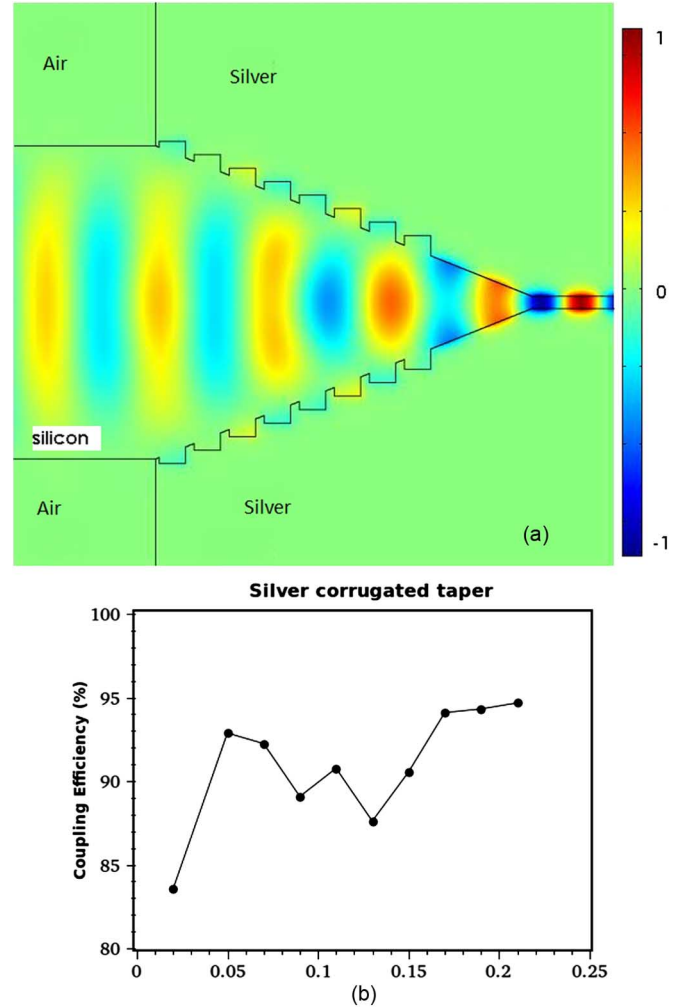


Fig. 4. (a)  $1.25 \mu\text{m}$  ( $w_1$ ) silicon slab to 50 nm ( $w_2$ ) silver plasmonic gap waveguide coupling with the same structure configuration shown in Fig. 3(b). The coupling efficiency is  $\sim 93\%$ ; the Hz field is plotted. (b) Plot of the coupling efficiency versus the plasmonic waveguide gap size.

smaller than  $2\lambda_{\text{spp,silver}} \approx 0.84 \mu\text{m}$  proposed in [18], [19] and the taper angle here is  $\sim 22^\circ$  (not  $58^\circ$  reported in [18], [19]). All facts point out again that the coupling mechanism of the corrugated waveguide reported in this work is different from those by exciting SPPs on metal surfaces depicted in [18], [19].

In summary, contrasted to [18], [19], the proposed corrugation (with period  $< \lambda_{\text{spp}}$ ) in the present work is more efficient in coupling light (slab guided mode) into the plasmonic  $\text{TM}_0$  mode for the silicon-based plasmonic metal-dielectric-metal structures. The high coupling efficiency is achieved through two main key points: (1) excellent mode matching to the plasmonic  $\text{TM}_0$  mode with  $\beta > k$  is made possible by the use of corrugation and (2) the corrugation only introduces very small loss since most of the fields in the corrugated part of the taper are still confined at the waveguide center. Instead, the corrugation (with period  $2\lambda_{\text{spp}}$ ) in [18], [19] is used for the excitation of SPPs with TM polarized light (not slab guided mode), which will introduce a larger amount of loss when the SPPs propagate on the grooved metal side walls.

### III. CONCLUSION

We have reported and designed a short ( $\sim 1.5 \mu\text{m}$ ) coupler for efficient light coupling between a silicon micro-slab and a nano metal-silicon-metal plasmonic waveguide based on the dispersion engineering of the “partially” corrugated waveguide structure for more precise mode matching. Numerical 87%  $\sim$  98% coupling efficiency for different gap sizes at the optical communication frequency is reported for the first time, which is comparable to or even higher than the previously referred performance of non-silicon and silicon based plasmonic gap waveguide coupling. These results should be very helpful for realizing full on-chip silicon plasmonic devices. We also point out that the coupling mechanism of the proposed structure in this work is different from those of [18], [19], which were achieved by exciting SPPs on grooved metal surfaces. Currently, the experiment is arranged for verification.

### ACKNOWLEDGMENT

The author would like to acknowledge Mr. Thompson, Mr. Gray from bp and Mr. Fwu from SGI for providing computing resources.

### REFERENCES

- [1] P. Ginzburg, D. Arbel, and M. Orenstein, “Gap plasmon polariton structure for very efficient microscale to nanoscale interfacing,” *Opt. Lett.*, vol. 31, pp. 3228–3230, 2006.
- [2] J. Wen, S. Romanov, and U. Peschel, “Excitation of plasmonic gap waveguides by nanoantennas,” *Opt. Exp.*, vol. 17, pp. 5925–5932, 2009.
- [3] G. Veronis and S. Fan, “Theoretical investigation of compact couplers between dielectric slab waveguides and two-dimensional metal-dielectric-metal plasmonic waveguides,” *Opt. Exp.*, vol. 15, pp. 1211–1217, 2007.
- [4] R. Yang, R. A. Wahsheh, Z. Lu, and M. A. G. Abushagur, “Efficient light coupling between dielectric slot waveguide and plasmonic slot waveguide,” *Opt. Lett.*, vol. 35, pp. 649–651, 2010.
- [5] G. L. James, “Analysis and design of TE<sub>11</sub>-to- HE<sub>11</sub> corrugated cylindrical waveguide mode converters,” *IEEE Trans. Microw. Theory Tech.*, vol. 29, pp. 1059–1066, 1981.
- [6] R. E. Collin, *Field Theory of Guided Waves*, 2nd ed. Piscataway, NJ, USA: IEEE Press.
- [7] K. Zhang and D. Li, *Electromagnetic Theory for Microwaves and Optoelectronics*, 2nd ed. New York, NY, USA: Springer, 2007.
- [8] R. Levy, “Tapered corrugated waveguide low-pass filters,” *IEEE Trans. Microw. Theory Tech.*, vol. 21, pp. 526–532, 1973.
- [9] Q. Gan, Z. Fu, Y. J. Ding, and F. J. Bartoli, “Ultrawide-bandwidth slow-light system based on THz plasmonic graded metallic grating structures,” *Phys. Rev. Lett.*, vol. 100, p. 256803, 2008.
- [10] A. Brimont, J. Vicente Galán, J. Maria Escalante, J. Martí, and P. Sanchis, “Group-index engineering in silicon corrugated waveguides,” *Opt. Lett.*, vol. 35, pp. 2708–2710, 2010.
- [11] A. I. Fernández-Domínguez, L. Martín-Moreno, F. J. García-Vidal, S. R. Andrews, and S. A. Maier, “Spoof surface plasmon polariton modes propagating along periodically corrugated wires,” *IEEE J. Sel. Topic Quantum Electron.*, vol. 14, pp. 1515–1521, 2008.

- [12] A. I. Fernández-Domínguez, L. Martín-Moreno, F. J. García-Vidal, S. R. Andrews, and S. A. Maier, “Spoof surface plasmon polariton modes propagating along periodically corrugated wires,” *IEEE J. Sel. Topic Quantum Electron.*, vol. 14, no. 6, pp. 1515–1521, 2008.
- [13] D. Martín-Cano, O. Quevedo-Teruel, E. Moreno, L. Martín-Moreno, and F. García-Vidal, “Waveguided spoof surface plasmons with deep-subwavelength lateral confinement,” *Opt. Lett.*, vol. 36, pp. 4635–4637, 2011.
- [14] N. F. Yu, Q. J. Wang, M. A. Kats, J. A. Fan, P. Khanna Suraj, L. Li, A. G. Davies, E. H. Linfield, and F. Capasso, “Designer spoof surface plasmon structures collimate terahertz laser beams,” *Nature Materials*, vol. 9, pp. 730–735, 2010.
- [15] A. M. B. Al-Hariri, A. D. Olver, and P. J. B. Clarricoats, “Low-attenuation properties of corrugated rectangular waveguide,” *Electron. Lett.*, vol. 10, no. 15, pp. 304–305, 1974.
- [16] M. Y. Chen and H. C. Chang, “Determination of surface plasmon modes and guided modes supported by periodic subwavelength slits on metals using a finite-difference frequency-domain method based eigenvalue algorithm,” *J. Lightw. Technol.*, vol. 30, pp. 76–83, 2012.
- [17] G. H. Bryant, “Propagation in corrugated waveguides,” *Proc. Inst. Elect. Eng.*, vol. 116, no. 2, pp. 203–213, 1969.
- [18] R. Thomas, Z. Ikonc, and R. Kelsall, “Silicon based plasmonic coupler,” *Opt. Exp.*, vol. 20, pp. 21520–21531, 2012.
- [19] G. Y. Li, C. Lin, X. Feng, and A. S. Xu, “Plasmonic corrugated horn structure for optical transmission enhancement,” *Chin. Phys. Lett.*, vol. 26, pp. 124205–12409, 2009.
- [20] A. D. Rakic, A. B. Djurišić, J. M. Elazar, and M. L. Majewski, “Optical properties of metallic films for vertical-cavity optoelectronic devices,” *Appl. Opt.*, vol. 37, pp. 5271–5263, 1998.
- [21] A. Mohammadi and M. Agio, “Dispersive contour-path finite-difference time-domain algorithm for modeling surface plasmon polaritons at flat interfaces,” *Opt. Express*, vol. 14, pp. 11330–11338, 2006.
- [22] G. Kewes, A. W. Schell, R. Henze, R. S. Schonfeld, S. Burger, K. Busch, and O. Benson, “Design and numerical optimization of an easy-to-fabricate photon-to-plasmon coupler for quantum plasmonics,” *Appl. Phys. Lett.*, vol. 102, p. 051104, 2013.
- [23] Y. Liu and K. Chang, “Nano-Optical Device Design With the Use of Open-Source Parallel Version FDTD and Commercial Finite Element Package,” arXiv: 1302.5489, 2013.

**Y. Liu** is currently with Department of Electrical and Computer Engineering, Texas A&M University, College Station, TX, USA.

Her research interests are plasmonic circuits, microwave circuits, integrated optics, and computational electromagnetics.

**Y. Lai** received the B.S.E.E. degree from National Taiwan University, Taipei, Taiwan, the M.S. and Ph.D. degrees from the Massachusetts Institute of Technology, Cambridge, MA, USA.

He is currently a faculty in Department of Photonics, National Chiao-Tung University, Hsinchu, Taiwan. The current research highlights of Professor Lai are microwave photonics, optical fiber communication, fiber optics, quantum optics and nonlinear optics.

**K. Chang** received the B.S.E.E. degree from National Taiwan University, Taipei, Taiwan, the M.S. degree from the State University of New York at Stony Brook, and the Ph.D. degree from the University of Michigan, Ann Arbor, MI, USA.

Prof. Chang is the Editor of the *Microwave and Optical Technology Letters* and the *Wiley Book Series in Microwave and Optical Engineering*.